AIMS Bioengineering

AIMS Bioengineering, 7(1): 29–42.
DOI: 10.3934/bioeng.2020003
Received: 07 November 2019
Accepted: 14 February 2020
Published: 17 February 2020

http://www.aimspress.com/journal/Bioengineering

Research article

A study into the fracture control of 3D printed intraosseous transcutaneous amputation prostheses, known as ITAPs

Joshua Bird, Euan Langford and Christian Griffiths*

College of Engineering, Swansea University, Swansea, UK

* **Correspondence:** Email: c.a.griffiths@swansea.ac.uk; Tel: +4407989687929.

Abstract: Amputated femurs traditionally have multiple health concerns, including the risk of infection. One way to mitigate this risk could be to use an intraosseous transcutaneous amputation prosthesis (ITAP), which is a way of attaching a prosthesis directly to the bone of the user. This paper attempts to customize an ITAP used in a transfemoral amputation so that it fails in a controlled manner, should failure be unavoidable. ABS specimens were 3D Printed and tested to understand how current designs fail. From these tests, an alternative design was developed. Simulations were conducted to insure the optimized design would withstand expected forces from walking. Titanium samples were then produced using additive manufacture and were subjected to tensile testing. These specimens incorporated a notch in the centre of the specimen to act as a stress concentrator. The design presented in this paper identified that the location of failure should move towards the prosthesis, and away from the femur. It was also shown that, titanium was found to have a greater breaking force than the femur; and is therefore not viable for use at this current stage.

Keywords: prostheses; ITAP; additive manufacture; tensile testing; notched specimen

1. Introduction

Traditional above-knee amputation prostheses use a stump and socket attachment. These products can lead to multiple health issues, including discomfort and bacterial infection [1,2]. Such problems can also limit the use of prostheses for users, further limiting their quality of life [1,2]. One possible way of minimizing the challenges associated with these prosthesis products is to use a transcutaneous prosthesis, which is attached directly to the bone. Direct skeletal implants have been used in dentistry to attach implants with over a 90% success rate [3]. One particularly promising area of research is the intraosseous transcutaneous amputation prosthesis, known as an ITAP. The ITAP has been inspired by deer antlers in that the protrusion has a tissue and bone interface that is not prone to infection [2]. To replicate this phenomenon, the new attachment design requires a flange immediately below the epithelial layer of skin to reduce the risk of infection and minimize tissue damage for amputees. The uptake of ITAP products must be based on evidence that they cause minimum harm to the user in both the long and short term. Therefore, for direct skeletal implants to be used in load-bearing bones, additional research to understand the loads which would cause an ITAP to fail need to be conducted. The main area of research covered in this paper is identify different ITAP design features which can result in a specified failure. For example, failure inside the femur could be catastrophic, possibly requiring further amputation and/or leading to infection. To avoid this, Newcombe et al. [4] suggest the space between the prosthesis and the bone anchor can be used for a fail-safe feature.

The ITAP has many possibilities to be customized to an individual; creating a bespoke design depending on the body weight and life style of the user. If the attachment is to be used in every-day life without inhibiting the user, it must withstand the forces *(F)* present in walking without failing. Thambyah et al. [5] found that approximately 3 times a person's body weight acts through the tibiofemoral joint when walking. Therefore, with no specific F acting on the joint, an ITAP design variation for people of different weights should be considered. Furthermore, the characteristics of the femur vary from person to person. Bone is made from cortical (dense, outer layer) and trabecular (spongy, cancellous, inner section) bone [6] and can be classified into 'organic' or 'mineral', phases [7]. In order for the ITAP to be inserted into the femur, it is assumed that the trabecular bone would be removed, and the prosthesis held in the center of the femur, held in place by the cortical bone surrounding it. Cortical bone can be described as elastic-brittle, and when tested under quasi-static loading, its resistance to a tensile F is lower than its resistance to a compressive F [8]. As the ITAP must fail without transferring excessive F to the bone; it is therefore required to break under a load which is less than the tensile F required to break the cortical bone.

The mechanical strength of a femur varies from person to person and depends on numerous factors. This can depend upon mineral content, age, and its porosity [9,10]. Furthermore, the porosity of the cortical bone also effects the fracture mechanics of the bone, as the pores act as local stress concentrations [11]. For example, an osteoporotic patient will suffer an increased risk of fracture compared with someone who does not [8]. When conducting research and simulations on the fracture of femurs, Marco et al. [12] summarized the mechanical properties of a femur, shown in Table 1. Furthermore, Reilly and Burstein [13] investigated the elastic and shear moduli of bone using human specimens, which are also outlined in Table 1.

Table 1. Mechanical properties of bone [12,13].

Mechanical property	Bone type	
	Trabecular	Cortical
Density (g/cm^3)	0.27	1.64
Young's modulus (MPa)	155	10,400
Shear modulus (MPa)	-	3,7100
Poisson's ratio	0.3	0.3
Failure strain	-	0.0165
Fracture toughness ($N/m^{0.5}$)	-	1549,214

Considering that the weight of the user is such a key factor in understanding the F the ITAP would be expected to withstand, and that every individual will have varying mechanical properties of bone, there is a need for customizing the design of the attachment to the individual. Modern manufacturing methods, such as 3D printing allow for bespoke designs to be manufactured that would otherwise be too difficult to produce with traditional machining methods [14]. However, it is important to note that the orientation of the print can affect the material properties; as that is not the topic of this report, the specimens must be printed such that the tensile force is parallel with the layers of the material [15]. As such bespoke designs may be required, it is possible that additive manufacture (AM) presents itself as a candidate manufacturing process that would be used in the production of direct skeletal implants in the future.

The focus of this paper is to explore the fracture mechanics of a fail-safe features on ITAP designs that have been produced via AM. In Section 2, current designs were tested under tensile loads to understand how they fail. These designs were manufactured using 3D printed acrylonitrile butadiene styrene (ABS). The ABS specimens were compared against simulated results to validate the use of finite element analysis (FEA) throughout this report. Using FEA, Two different fail-safe features were tested; a 'necked' design, where the diameter of the exposed region of the ITAP is continuously reduced to the mid-point, and then increased again up to the prosthesis, and a 'notched' design, which has a constant diameter, with a stress-raiser in the center of the exposed section. In Section 3, the notched fail-safe feature was subject to further simulations using ANSYS which were used to test different notches, to ensure the ITAP would withstand the expected F associated with the user walking. In Section 4; titanium (Ti) specimens with a notch, which acted as a stress concentration, were produced using AM, and subject to tensile testing to understand if it would be a suitable material for producing the optimized designs [16]. Ti was chosen as the test material as it is commonly used in biomedical applications and can be readily used in AM processes [17].

2. Experimental methodology

2.1. Preliminary testing and simulations

Preliminary tests were required to understand how and where current designs of ITAP fail, in order to redesign the exposed region appropriately, to ensure any failure is away from the femur. In order to accurately model the ITAP, 3D printing was used to allow the complex geometry of the prosthesis were manufactured. Tensile tests were conducted on the 3D printed specimens and their results are displayed in Table 2. These tests could be used to compare simulated results to ensure that the ITAP would withstand expected walking loads.

Table 2. Locations of failure and F in initial testing.

F at failure (N)	Location of failure
3901.66	flange only
3681.67	flange and 3.6 mm (avg) towards the bone from flange

These tests required an initial ITAP to be modelled and manufactured. Transfemoral amputations may be required at any point along the length of the femur [18]. Newcombe et al. [4] designed four different length ITAPs depending on the resected length of the bone. The designs, however, all used a 140 mm insert to go into the bone which was 14 mm in diameter. Devinuwara et al. [19] state that the optimal transfemoral amputation leaves a 120 mm clearance above the fulcrum of the contralateral lower limb. These three dimensions were used to model an initial ITAP, which was 3D printed in ABS, as shown in Figure 1. These specimens were printed with 100% infill on a stratasys objet 1000 fused deposition modelling 3D printer. They were printed horizontally to ensure that the specimens did not collapse during manufacture, and that the layers were parallel to the tensile force [15,20]. These 3D printed ITAPs were subjected to tensile loads using a hounsfield 50 kN tensile testing machine [21] shown in Figure 2. The specimens were displaced at a rate of 3 mm/min, in line with British Standards [22] They were subjected to a *F* until the specimens failed in order to establish how the current designs fractured, as shown in Figure 2. Table 2 highlights the results from the initial tests.

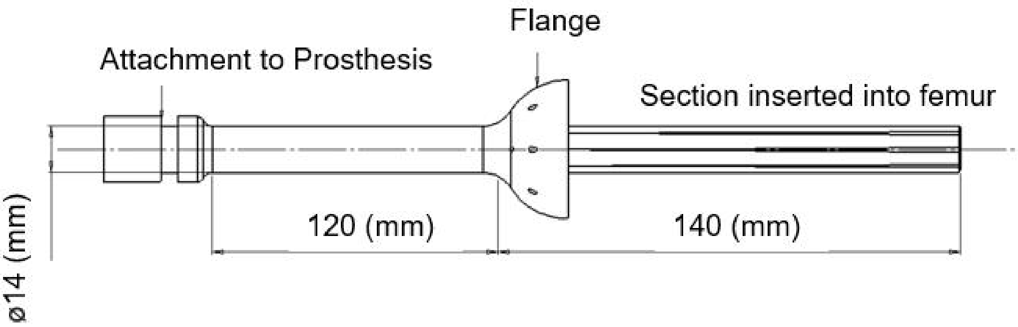

Figure 1. Current ITAP design [4,17].

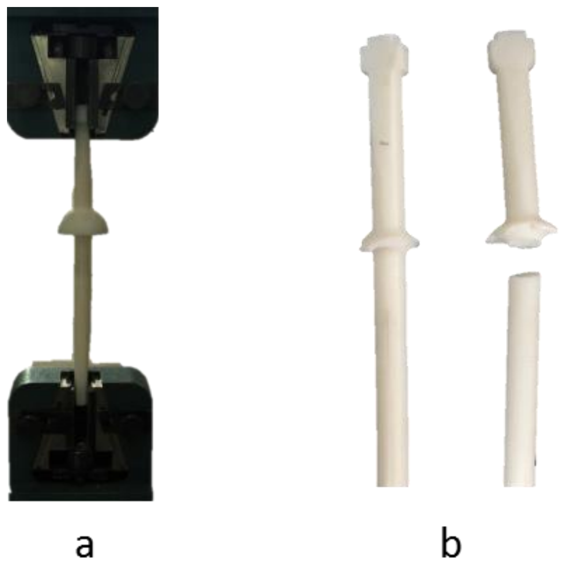

Figure 2. The preliminary test set-up (a) and the failed specimens (b).

The most important information from these preliminary tests is the ‘location of failure’ as this shows where the present ITAP designs fail. Table 2 shows that when subjected to a tensile load, the ITAP failed at the flange in both tests. In the first test, only the flange failed, and in the second test, the shaft failed approximately 3.6 mm towards the bone-side of the ITAP, from the flange. Following the preliminary tensile tests, initial stress (σ) analysis simulations were conducted. These simulations used a simplified model of the ITAP, to confirm if the FEA would show a similar point of failure compared with the tensile test results from Table 2. The simplified model did not feature any 'human' sections in the tests, but assumed that the section of the ITAP which would be inserted into the femur was fixed, and *F* were applied where the prosthesis would be attached. The *F* used for the initial simulations were based on an average body weight of 67 kg. For the preliminary simulations it was assumed that the ITAP was fixed in the bone. As shown in Figure 3a, the simulations showed the σ concentrated approximately at the flange which is a very similar location to the preliminary tensile tests.

As the preliminary experiments and the initial simulations both showed failure around the location of the flange, it can be assumed that all simulations conducted would also be comparable to physical testing. Two different alternative fail-safe designs of ITAP were then simulated, a 'notched' design, and a 'necked' design, shown in Figure 3b and Figure 3c respectively. The 'notched' design has a σ concentrating notch in the center of the exposed section of the ITAP (Figure 3b). The alternative 'necked' design includes a continuously reduced diameter to the mid-point of the ITAP, which then then increases up to the prosthesis (Figure 3c). A maximum diameter of 14 mm was used in every model. Both the notched and necked designs were simulated with minimum diameters of 5 and 10 mm. The simulations indicated that both designs have high areas of σ at approximately the center of the exposed region of ITAP, shown in Figure 4. However, the notched designs have a concentration towards the attachment to the prosthesis; whereas the σ concentration in the necked design is closer to the bone. Figure 4 shows how the *σ* varies along the necked and notched designs with a 10 mm minimum diameter respectively.

The FEA results in Figure 4, show the variation of σ increases consistently as the diameter of the ITAP decreases, this is not ideal for controlled fracture as it does not offer a singular focused area of σ. The maximum stress (σ_{max}) of the notched design is approximately 1.38 times greater than the σ_{max} the necked design undergoes. Furthermore, it does not increase linearly along the length of the ITAP, but there is a sudden increase in σ in the area of the notch, as seen in Figure 4. The σ_{max} in the notched design is approximately 5 mm further away from bone than the σ_{max} in the necked design.

Considering that the notch caused a sudden increase in the σ_{max} along the specimen, and that it would cause failure approximately 5 mm further away from the femur, and towards the attachment to the prosthesis only the notched design was chosen for further development and analysis in Section 2.2.

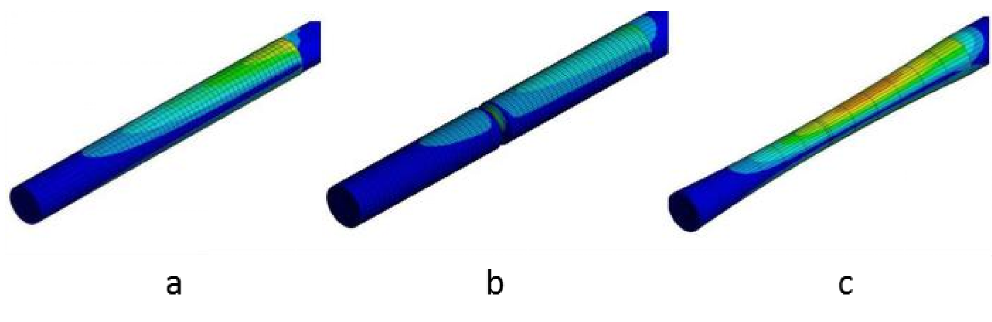

Figure 3. Simulations using ANSYS to test the (a) standard design (b) notched design and (c) necked design.

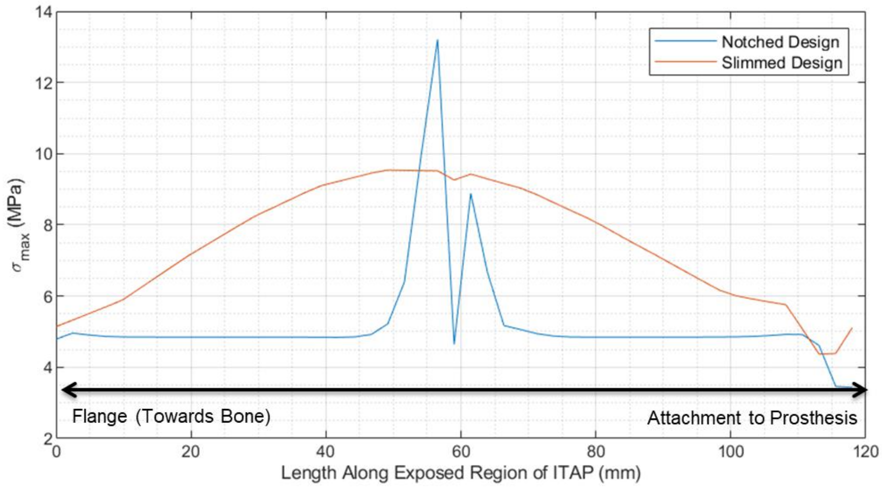

Figure 4. Stress along the length of the exposed section of the ITAP.

2.2. Simulations under expected walking forces

To ensure the prosthesis attachment would break without compromising the bone more realistic simulations were conducted. The optimised model includes a human femur in the simulations, and the mechanical properties of bone were applied to the computational model. The information from Table 1 was used to conduct advanced simulations under normal walking *F*. The expected walking *F* is then used to identify the areas of σ_{max} under normal conditions.

If the ITAP is to be used in every-day life without inhibiting the user, it must withstand *F* present in walking, when approximately 3 times a person's body weight acts through the tibiofemoral joint. Using the maximum forces ($F_{\max}$) that three human knee joints went through when walking [5], a vertical compressive force (F_y) and a proportional shear force (F_x) were applied to the exposed end of the model. The mechanical properties of cortical bone from Table 1 were applied to the model in a simplified femur, and the outer layer was fixed. This was carried out with the assumption that the femur would be held in situ by the surrounding muscle. The ITAP was then tested with the designed failure feature. In particular, the following were investigated; no notch (i.e. minimum diameter of 14 mm), and 13 down to 2 mm minimum diameter, in 1 mm increments. The equivalent σ in the ITAP was measured in each iteration. In all the simulations, the σ_{max} was present in the notched area apart from the no notch simulation. The σ_{max} and displacements from each simulation are shown in Table 3. The results show that the 2 and 3 mm minimum diameters cannot be used, as the specimen failed under expected *F*. Furthermore, Table 3 indicates that the ITAP should withstand expected loads in daily use, as long as the notch in the exposed region is no smaller than 4 mm.

The σ_{max} measured was then compared with the minimum diameter. The 2 and 3 mm diameters were omitted as they failed in the simulations. Figure 5 shows the relationship between the diameter and σ_{max}. For the maximum and average walking loads, σ_{max} increases up to 5 mm, then decreases. This pattern is observed at 4 mm in the minimum walking load case. This is likely due to the relationship between σ, the cross-sectional area (A), and *F*; given that *F* is directly proportional to σ, whereas A is inversely proportional to σ. This implies that when σ increases, *F* is the dominant parameter on the specimen; whereas when σ decreases A is the dominant parameter.

Table 3. The σ_{max} and maximum displacement in the ITAPs found in the iterative simulations, with different compressive (F_y) and shear (F_x) forces.

Notch root diameter (mm)	Test 1		Test 2		Test 3	
	F_y of 2075 N, F_x of 186 N		F_y of 1900 N, F_x of 95 N		F_y of 2250 N, F_x of 190 N	
	σ_{max} (MPa)	displacement (mm)	σ_{max} (MPa)	displacement (mm)	σ_{max} (MPa)	displacement (mm)
14	99.1	0.831	56.6	0.435	102.2	0.851
13	114.3	0.833	70.0	0.435	118.6	0.852
12	155.4	0.834	95.0	0.438	161.2	0.857
11	216.9	0.847	131.9	0.443	224.9	0.867
10	234.4	0.856	142.2	0.444	242.9	0.879
9	299.3	0.880	178.9	0.456	309.8	0.900
8	429.3	0.922	253.6	0.478	443.9	0.943
7	578.3	0.990	336.9	0.512	597.2	1.012
6	795.3	1.111	456.4	0.574	820.2	1.136
5	1329.2	1.359	750.6	0.700	1368.9	1.389
4	1104.5	1.997	1174.5	0.978	1119.9	2.016
3	Failed		1171.8	1.814	Failed	
2	Failed		Failed		Failed	

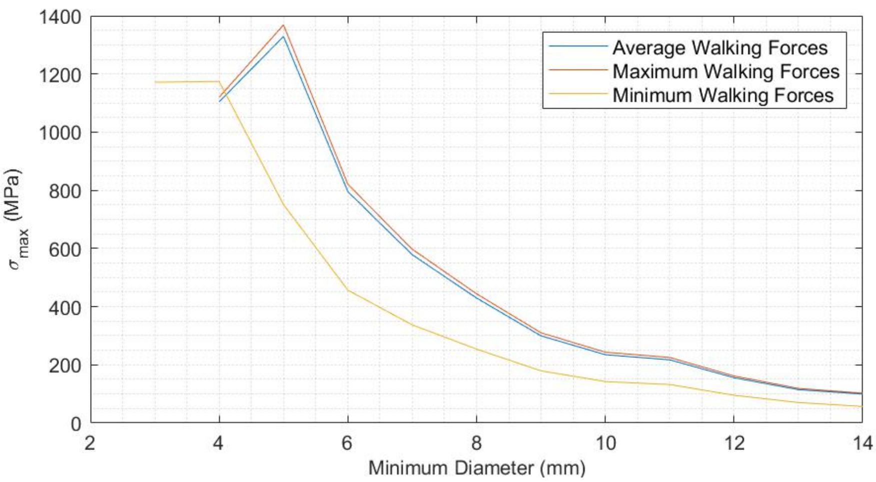

Figure 5. σ_{max} for different notch root diameters under walking forces.

2.3. Manufacture of titanium specimens and testing

As outlined in Section 2.1, the ITAP should withstand the expected loads associated with walking, as long as the attachment does not have a notch with a minimum diameter of under 4 mm. However, the notch should focus failure away from the bone when subject to an excessive load. This failure should be caused by a load less than the F_{max} that a femur can withstand. Mather [23] found that the average F required to break the femur of a male is approximately 3.2 kN, and to break the femur of a female is approximately 2.2 kN. Ti specimens were produced using AM to verify if the material and manufacturing technique can be used to produce customized ITAPs. The Ti specimens to be printed were selected based on the results in Figure 5 and diameters of 13, 9, and 5 mm were chosen, as these represent a wide range of σ_{max}. Ti is currently used in medical applications as it is widely bio-compatible, and therefore was chosen for testing [10]. Due to the limitations of the selective-laser melting (SLM) machine available, the height of the specimens had to be reduced. As such, the required dimensions for the sample were calculated using British Standard ratios [24]. The diameters of the samples had to be reduced to use the SLM machine, shown in Figure 6. Therefore, all subsequent discussion shall refer to specimens by the percentage reduction in diameter; the 13, 9, and 5 mm specimens had a percentage reduction in diameter of 7% 36% and 64% respectively. The samples were tensile tested on a hounsfield 50 kN tensile testing machine, at a rate of 3 mm/min. This displacement speed was chosen to ensure the tests were comparable with the preliminary experiments conducted in Section 2.1. The vertical tensile force (F_t) and displacement were sampled every 0.5 s. The failed specimens are shown in Figure 7.

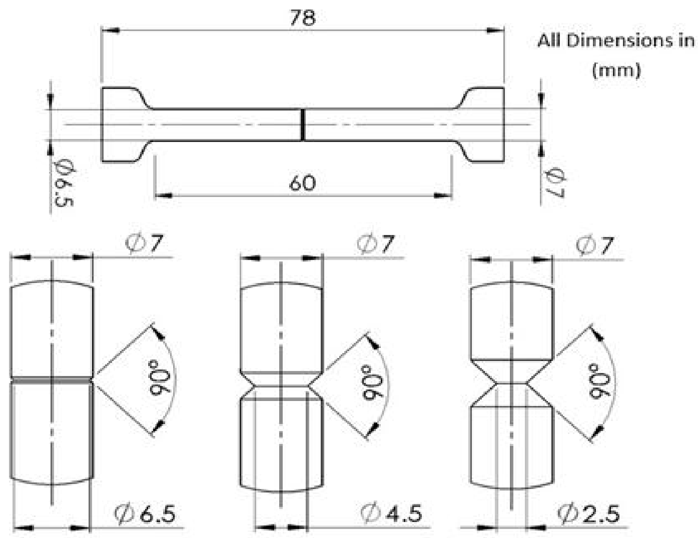

Figure 6. From left to right: diameter reduction of 7%, 36% and 64%.

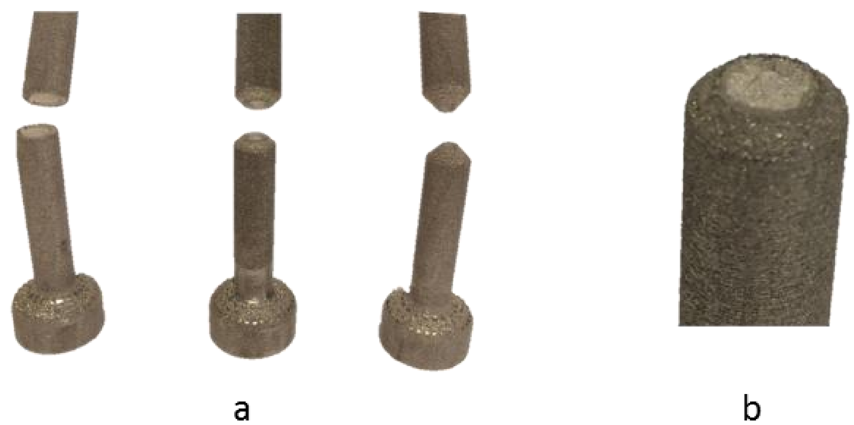

Figure 7. Example samples after testing (a) from left to right diameter reduction of 7%, 36% and 64% (b) face of the fractured surface on the 36% specimen.

2.4. Tensile testing results

All the specimens failed in the notched region, as shown in Figure 7. The F against displacement curves for each of tested specimens tested are shown in Figure 8, which shows that introducing a notch diameter can cause consistent failure in the specimen. The 7% reduction specimens failed at approximately 41 kN, and the 64% specimens failed at 8–9 kN. There was more variation observed in the 36% reduction specimens, which failed at approximately 17 kN, with one specimen failing at 19 kN and another specimen failing at 21 kN.

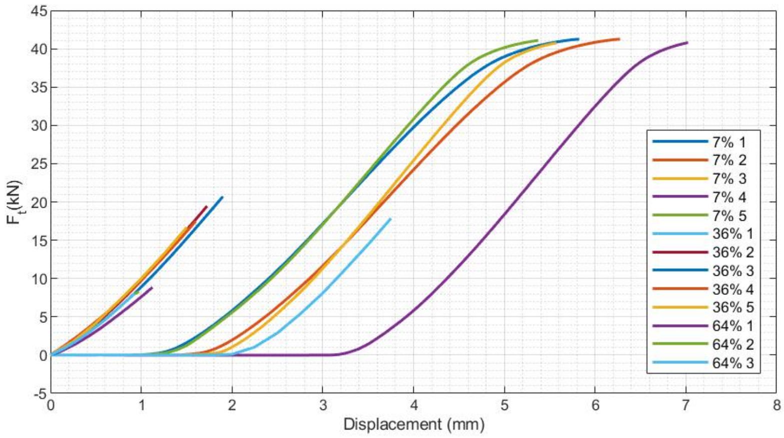

Figure 8. Force against displacement for all tensile tested specimens.

The specimens exhibited 'mode 1' failure, whereby the crack propagates perpendicularly to the applied F [25]. Figure 7 b shows the face of the fractured 7% specimen, where it can be seen that there is a very small cup, indicative of ductile failure. This is apparent in the stress-strain graphs in Figure 9, where all the specimens underwent brittle failure apart from the 7% specimen curves which show a small change in gradient prior to failure. Additionally, Figure 10 shows the stress-time graphs for all of the specimens. The accelerated failure in the 7% specimens suggests that they underwent a minimal amount of ductile behavior prior to failure. However, once the specimen had started to neck, the specimen failed rapidly. This suggests that the notch causes an accelerated failure once the crack starts to propagate, which appears as a brittle failure on the stress-strain curves, and as an accelerated failure on the 7% specimens.

This is because the notch acts as a σ concentration [26], and the reduced diameter increases the σ in that region. If the stress is raised by the notch such that the ultimate tensile load (UTL) the specimen can undergo before it fails is reduced to below the Elastic Limit (EL) of the material, the notched specimen will fail before it can plastically deform. The EL is the σ that will start to cause plastic deformation, which for a Ti specimen is approximately 600–880 MPa for machined or sintered Ti [27,28] and for SLM specimens the EL is approximately 400 MPa [29]. Over a σ of 400 MPa, the specimen would start to exhibit plastic deformation prior to failure, whereas any failure beneath this limit would be considered as an accelerated failure.

Thus, introducing a notch into the specimen reduces the EL that Ti can undergo significantly, reducing the UTL to below the EL. This can be seen in Figure 9, where all the specimens failed at a σ below 400 MPa. The varying gradient in the 7% specimens suggests that the specimens yielded;

this can be attributed to a ductile behavior. However, as this ductile region is very minimal compared with the brittle region, and as the specimens all failed below 400 MPa, this can still be considered as brittle failure.

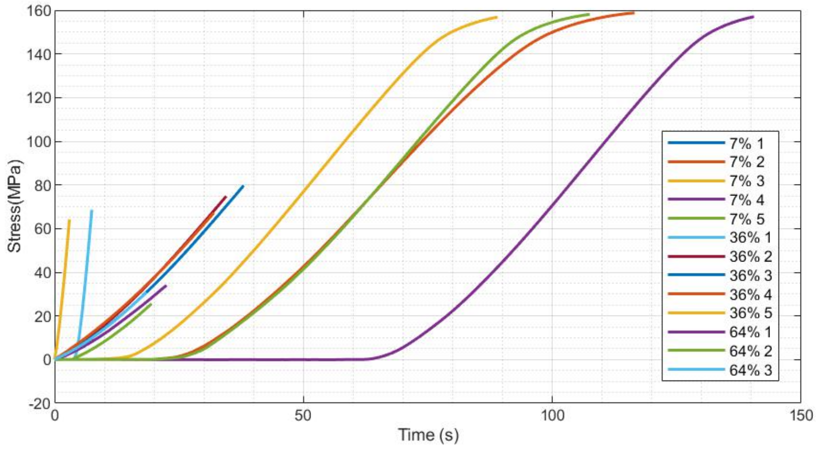

Figure 9. Stress against strain for all tensile tested specimens.

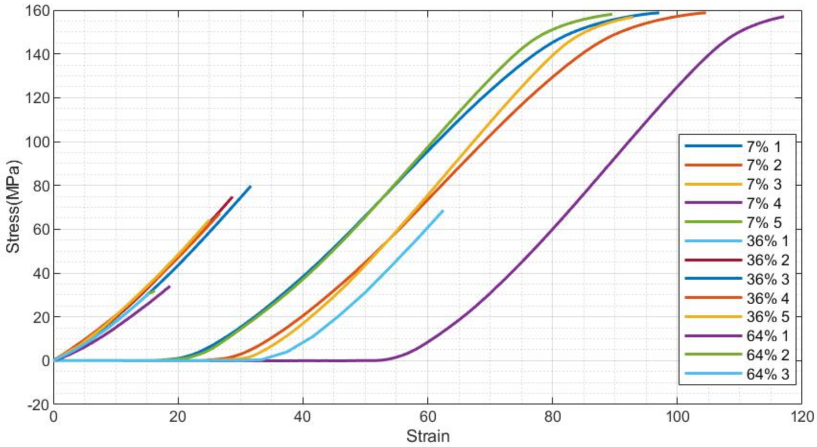

Figure 10. Stress against time for all tensile tested specimens.

Reducing the UTL of the ITAP by introducing a notch is comparable to introducing a σ raiser; which focusses the σ into a specific area of the specimen [30]. The effect of different defects or cracks in a material can be measured using σ concentration factors [26,31]. A σ concentration factor indicates how different σ-raising geometric features will affect a material [30,32]. The theoretical σ intensity factor for a cylindrical specimen with a 'V'-shaped notch is given by Equation 1. This in turn can be used in Equation 2 to calculate the σ at an 'infinite' distance away from the notch, σ_{yy}.

$$K_{t\theta} = 1.065K_{tu} - \left[0.022 + 0.137\left(\frac{\theta}{135}\right)^2\right](K_{tu} - 1)K_{tu} \tag{1}$$

$$\sigma_{yy} = \frac{K_{t\theta}}{\sqrt{2\pi r}} \tag{2}$$

Where $K_{t\theta}$ is the stress intensity factor in a 'V' notched specimen compared with K_{tu} is the factor caused by a 'U'-shaped notch. The angle of the notch in the equation is θ, and r is the length of the crack [30].

Equation 2 indicates that the greater the length of the crack, the lower the σ_{max}, a specimen can undergo prior to failure. This is also observed in Figure 6 as the diameter is reduced, the specimen's resistance to force is also reduced. Whilst this demonstrates that the smaller the notched diameter, the weaker the sample becomes; it is still too strong to be implanted into a femur. The 68% reduced diameter specimens failing at 7 kN without scaling the F to be applicable for a full-sized ITAP, whereas the femur has a UTL of 2.2–3.2 kN, as such the femur would fail before the ITAP. Therefore, the chosen material is too strong for purpose. If the ITAP were to undergo a F strong enough to fail, the femur would already have failed. This suggests that the modified design is 'over-engineered', despite moving failure away from the femur. However, if a material with a lower tensile strength was used to manufacture the ITAP, this may not be the case. Further research into different materials would be beneficial to understand if the notched design creates enough of a σ-concentration.

3. Conclusions

The potential of the ITAP method of attaching a prosthesis directly to the bone of the user could be a step to improving the quality of life for amputees. The investigated designs considered a functional ITAP with a fail-safe method that included a notch design that prevents possible damage to the user's bone. The results show that a combination of Ti and the notched design cannot currently be used as a fail-safe as the Ti material has a significantly higher UTL and EL compared with a femur. This means that the femur would break or shatter before the ITAP would fail and that the prosthesis attachment could break the bone it is anchored to. Currently, the health risks and discomfort of a stump and socket attachment are minimal compared with the risk of breaking the bone, which could make further amputation necessary. Further development, using a different material should be conducted to ensure failure at a lower force than the UTL of a femur. Alternatively, Ti could continue to be the subject of research using a different modified design of ITAP, potentially using a generative design to produce the weakened model, where only the structural material is necessary to ensure that it would not break under walking loads. The main findings from the research are as follows:

- Current ITAP designs risk failure near the flange, and could risk damaging the user's body, specifically the femur, and the skin at the boundary of the amputation.
- The notch in the additively manufactured titanium ITAP reduces the ultimate tensile load the specimen can undergo to below the elastic limit of machined or even SLM titanium with no notch. This can be exploited to cause controlled fracture outside the femur, and in the exposed region of the ITAP.
- Introducing a notch into the exposed region of the ITAP could induce failure in a manner which does not cause harm to the user when compared with failure inside the femur. However, this notch does not inhibit everyday use, as the ITAP can still be used for walking, and will

withstand expected forces.

- Titanium is too strong a material to be used in the ITAP with the current designs researched. Results show that it will break under a force greater than a force required to break a femur. Further designs could be researched so that the bone would have a higher ultimate tensile load compared with the ITAP.

Further research is recommended to better the design for bespoke use depending on the lifestyle of the user. This may include studying the forces and loading associated with different activities, such as running and jumping, or side-ways movements. Further research should also look at the shear forces associated with a sudden extreme load. Repeat loading should also be studied, to understand how the notched region or further design iterations withstand walking loads over time, and if there is any wear due to repeat and constant cyclic loading.

Acknowledgments

The authors would like to acknowledge the support of the Future Manufacturing Research Institute, College of Engineering, Swansea University and Advanced Sustainable Manufacturing Technologies (ASTUTE 2022) project, which is partly funded from the EU's European Regional Development Fund through the Welsh European Funding Office, in enabling the research upon which this paper is based. Further information on ASTUTE can be found at www.astutewales.com.

Conflict of interest

The authors declare no conflict of interests.

References

1. Tranberg R, Zügner R, Kärrholm J (2011) Improvements in hip-and pelvic motion for patients with osseointegrated trans-femoral prostheses. *Gait Posture* 33: 165–168.
2. Pendegrass CJ, Goodship AE, Price JS, et al. (2006) Nature's answer to breaching the skin barrier: an innovative development for amputees. *J Anat* 209: 59–67.
3. Albrektsson T, Jansson T, Lekholm U (1986) Osseointegrated dental implants. *Dent Clin North Am* 30: 151–174.
4. Newcombe L, Dewar M, Blunn GW, et al. (2013) Effect of amputation level on the stress transferred to the femur by an artificial limb directly attached to the bone. *Med Eng Phys* 35: 1744–1753.
5. Thambyah A, Pereira BP, Wyss U (2005) Estimation of bone-on-bone contact forces in the tibiofemoral joint during walking. *Knee* 12: 383–388.
6. Rho JY, Kuhn-Spearing L, Zioupos P (1998) Mechanical properties and the hierarchical structure of bone. *Med Eng Phys* 20: 92–102.
7. Willett TL, Dapaah DY, Uppuganti S, et al. (2019) Bone collagen network integrity and transverse fracture toughness of human cortical bone. *Bone* 120: 187–193.
8. Bettamer A, Hambli R (2016) *Finite Element Simulation of Fracture Profile of Bone Material: A Case of Study Applied to Human Femur Specimen*. Elsevier.

9. Zioupos P, Currey JD (1998) Changes in the stiffness, strength, and toughness of human cortical bone with age. *Bone* 22: 57–66.
10. Currey JD (2010) Mechanical properties and adaptations of some less familiar bony tissues. *J Mech Behav Biomed* 3: 357–372.
11. Iori G, Heyer F, Kilappa V, et al. (2018) BMD-based assessment of local porosity in human femoral cortical bone. *Bone* 114: 50–61.
12. Marco M, Giner E, Larraínzar-Garijo R, et al. (2017) Numerical modelling of femur fracture and experimental validation using bone simulant. *Ann Biomed Eng* 45: 2395–2408.
13. Reilly DT, Burstein AH (1975) The elastic and ultimate properties of compact bone tissue. *J Biomech* 8: 393–405.
14. Griffiths CA, Howarth J, De Almeida-Rowbotham G, et al. (2016) A design of experiments approach to optimise tensile and notched bending properties of fused deposition modelling parts. *Proc IMechE Part B: J Engineering Manufacture* 230: 1502–1512.
15. Tanoto YY, Anggono J, Siahaan IH, et al. (2017) The effect of orientation difference in fused deposition modeling of ABS polymer on the processing time, dimension accuracy, and strength, *AIP Conference Proceedings* 1788: 030051.
16. Murr LE, Gaytan SM, Ramirez DA, et al. (2012) Metal fabrication by additive manufacturing using laser and electron beam melting technologies. *J Mater Sci Technol*: 1–14.
17. Chen Y, Frith JE, Dehghan-Manshadi A, et al. (2017) Mechanical properties and biocompatibility of porous titanium scaffolds for bone tissue engineering. *J Mech Behav Biomed* 75: 169–174.
18. Zheng L, Luo JM, Yang BC, et al. (2005) 3D finite element analysis of bone stress around distally osteointegrated implant for artificial limb attachment. *Key Eng Mater* 288–289: 653–656.
19. Devinuwara K, Dworak-Kula A, O'Connor RJ (2018) Rehabilitation and prosthetics post-amputation. *Orthop Trauma* 32: 234–240.
20. Langford E, Griffiths CA (2018) The mechanical strength of additive manufactured intraosseous transcutaneous amputation prosthesis, known as the ITAP. *AIMS Bioeng* 5: 133–150.
21. Tinius Olsen, Frame Capacities from 1 to 50 kN (200-11k Ibf), 2017. Available from: https://www.tiniusolsen.com/tinius-olsen-products/tensile-compression-tinius-olsen/st-series.
22. Plastics. Determination of tensile properties. General principles. BS EN ISO 527-1, 2019. Available from: https://bsol.bsigroup.com/Bibliographic/BibliographicInfoData/000000000030377399.
23. Mather BS (1968) Variation with age and sex in strength of the femur. *Med Biol Eng* 6: 129–132.
24. Metallic materials. Tensile testing. Merhod of test at room temperature. BS EN ISO 6892-1, 2019. Available from: https://bsol.bsigroup.com/Bibliographic/BibliographicInfoData/000000000030395181.
25. Chang KH (2013) *Product Performance Evaluation using CAD/CAE: The Computer Aided Engineering Design Series*, New York: Academic press.
26. Irwin GR, Paris PC (1971) Fundamental aspects of crack growth and fracture, In: Liebowitz H, *Engineering Fundamentals and Environmental Effects*, New York: Academic Press, 1–46.
27. Welsch G, Boyer R, Collings EW (1993) *Materials and Properties Handbook: Titanium Alloys*, USA: ASM international.

28. Niinomi M, Liu Y, Nakai M, et al. (2016) Biomedical titanium alloys with Young's moduli close to that of cortical bone. *Regen Biomater* 3: 173–185.
29. Attar H, Bermingham MJ, Ehtemam-Haghighi S, et al. (2019) Evaluation of the mechanical and wear properties of titanium produced by three different additive manufacturing methods for biomedical application. *Mater Sci Eng* 760: 339–345.
30. Young WC, Budynas RG, Sadegh AM, et al. (2002) *Roark's Formulas For Stress and Strain*, New York, McGraw-Hill.
31. Barenblatt GI (1962) The mathematical theory of equilibrium cracks in brittle fracture, In: Dryden HL, Kuerti G, Van den Dungen FH, *Advances in Applied Mechanics*, New York: Academic Press, 55–129.
32. Newman Jr JC, Raju IS (1981) An empirical stress-intensity factor equation for the surface crack. *Eng Fract Mech* 15: 185–192.

AIMS Press

© 2020 the Author(s), licensee AIMS Press. This is an open access article distributed under the terms of the Creative Commons Attribution License (http://creativecommons.org/licenses/by/4.0)